CHEMICAL ENGINEERING TRANSACTIONS

VOL. 103, 2023

A publication of AIDIC
The Italian Association of Chemical Engineering
Online at www.cetjournal.it

Guest Editors: Petar S. Varbanov, Panos Seferlis, Yee Van Fan, Athanasios Papadopoulos

ISBN 979-12-81206-02-1; **ISSN** 2283-9216

DOI: 10.3303/CET23103010

Condensation Characteristics of Flows in Newly Developed, Three-Dimensional Enhanced Heat Transfer Tubes

David J. Kukulka[a,*], Rick Smith[b], Wei Li[c]

[a]State University of New York College at Buffalo, 1300 Elmwood Avenue, Buffalo, New York, 14222 USA,
[b]Vipertex, 658 Ohio Street, Buffalo, New York. USA
[c]Department of Energy Engineering, Zhejiang University, 866 Yuhangtang Road, Hangzhou 310027, China
kukulkdj@buffalostate.edu

Condensation heat transfer characteristics were studied experimentally to evaluate the heat transfer performance for copper heat transfer tubes (smooth and enhanced). Condensation tests were performed at 45 °C (saturation temperature); mass flux values in the range of 50 to 400 kg/(m^2·s), with an inlet vapor quality of 0.8 and outlet vapor quality of 0.2. Single-phase heat balance verification found that the heat loss is less than 6 %, and the deviation between single-phase experimental results and various prediction correlations is less than 15 %. The condensation heat transfer coefficient increases with an increase in mass flow. When the mass flow rate increases, the turbulence of the liquid flow increases, and the liquid film becomes thinner; thermal resistance is reduced, and the heat transfer coefficient increases. Heat transfer values at lower mass velocities increase slightly with increasing mass flux values; however, at higher mass flux rates, the heat transfer increase is larger than that at low mass flux values. Experimental results determined that the performance factor ratio for most tubeside and outside condensation heat transfer conditions (enhanced tube/smooth tube) of the three-dimensional surfaces investigated in this study are greater than 1.

1. Introduction

With the recent development of enhanced three-dimensional tubes, studies of condensation have become important topics to study. Li et al. (2017) evaluated the condensation heat transfer characteristics in micro-finned tubes and compared performance with smooth tubes. Kukulka et al. (2014) experimentally evaluated tubeside condensation heat transfer for various enhanced tubes; Kukulka et al. (2019) presented HTC and frictional pressure drop data for condensation heat transfer on the outside of enhanced three-dimensional tubes. Li et al. (2020) compared the heat transfer performance of several stainless steel-enhanced tubes. Kukulka et al (2022) presented visual flow patterns and heat transfer performance for flow condensation. Gu et al. (2020) evaluated the condensation heat transfer of moist air outside three-dimensional finned tubes experimentally. Tang et al. (2020) compared the condensation flow pattern in a three-dimensional enhanced tube and detailed the transition position. Diani et al. (2018) investigated the condensation of a 4 mm (OD) helix micro fin tube. They found that when the vapor quality is less than 0.7, the correlation between vapor quality and HTC is positive. However, fluctuations in pressure drop were seen. Additionally, when the vapor quality is greater than 0.7, the HTC is no longer positively related to increasing vapor quality; and for increasing vapor quality, there is an increase in pressure drop.
An experimental study of condensation heat transfer and flow characteristics in corrugated tubes (using R134a) was performed by Laohalertdecha and Wongwises (2011). Zhang et al. (2018) conducted experiments in order to determine the effects of saturation temperature on the condensing heat transfer characteristics (when using R410A) inside smooth and micro-fin tubes. Their results indicate that a higher heat transfer coefficient was found at a lower saturation temperature; this is due to the lower vapor density, higher liquid thermal conductivity, and higher surface tension. Finally, the enhanced effects of micro-fins were analyzed, and existing correlations were compared.
Several studies have evaluated the effect of tube thermal conductivity, tube diameter, and tube shape on heat transfer performance. Zhao et al. (2017) studied the influence of surface structure and tube thermal conductivity

Paper Received: 14 April 2023; Revised: 05 June 2023; Accepted: 21 July 2023
Please cite this article as: Kukulka D.J., Smith R., Li W., 2023, Condensation Characteristics of Flows in Newly Developed, Three-Dimensional Enhanced Heat Transfer Tubes, Chemical Engineering Transactions, 103, 55-60 DOI:10.3303/CET23103010

on the condensation HTC inside enhanced 2D and 3D finned tubes made of iron cupronickel and aluminum brass. They concluded that: (i) The use of enhanced surface structures produces larger HTC increases when using R410A than when using R134a ; (ii) Tubes with higher thermal conductivities produce larger condensation HTC values than tubes produced from lower thermal conductivity materials; (iii) A 3D finned surface has larger condensation HTC values than a 2D finned surface; (iv) Tube material thermal conductivity produces different subcooling temperature distributions in the fins and affects the condensation heat transfer performance.

For the design, development, and assessment of high-performance heat transfer systems, heat transfer performance data of three-dimensional tubes is important. To determine how well three-dimensional enhanced tubes transfer heat, an experimental study is necessary. Smooth and three-dimensional tubes (5EHT and HB/D) will be evaluated in this paper. According to Webb et al. (2005), three-dimensional enhanced tubes can increase surface area, promote fluid mixing, generate secondary flows, create boundary layer separation, and increase turbulence intensity; all these factors make three-dimensional enhanced tubes an important consideration when evaluating alternatives to improve heat transfer. Kukulka et al. (2013) investigated various EHT-enhanced tubes, and single-phase results show heat transfer performance of the EHT-enhanced tubes was improved by more than 500 %. These tubes produced an earlier transition to turbulence, occurring approximately when the Reynolds number was near 1,000. Additionally, the enhanced structure also produces a more intense disturbance to the two-phase flow interface and disrupts the boundary layer.

There is a lack of heat transfer data concerning 3D enhanced tubes; this study adds to the knowledge base of three-dimensional heat transfer tubes. Modifying the surface structure of a tube is a passive enhancement method; for the surface designs considered here, there is a lack of performance data; in order to advance these enhanced tube designs, experimental performance analysis must take place. For the design, development, and assessment of high-performance heat transfer systems, heat transfer/pressure drop data of three-dimensional tubes is presented. Previously there have been theoretical studies and some experimental studies that studied some tubes. However, it is difficult to rely solely on a theoretical analysis or only a numerical analysis in order to determine performance in enhanced tubes. In order to determine how well these enhanced tubes conduct heat and how they affect condensation heat transfer, an experimental study is necessary. Additionally, in order to utilize enhancement results in industrial designs, an accurate engineering model must be obtained, currently, heat transfer performance (tubeside and outside of the tube) data is lacking for these types of enhanced tubes. Experimental research has been performed to determine the heat transfer performance of smooth, herringbone microgrooves with a dimple (HB/D), and three-dimensional (5EHT) tubes over a wide range of conditions; condensation heat transfer performance (tubeside and outside the tube) is discussed. This study presents new results since previous studies have not addressed the conditions for the three-dimensional surfaces evaluated here.

2. Experimental details

Figure 1 details the experimental apparatus used in this study. Images of the enhanced surfaces studied here are presented in Figure 2. When tube side condensation is studied, the test section (as can be seen in Figure 1) of the apparatus is composed of a horizontal counter-flow heat exchanger; refrigerant flows in the enhanced tube being evaluated, and cooling water is flowing in the external annular casing of the enhanced tube. After the test section, the cooling water is measured using a mass flowmeter and returned to the constant temperature water tank; here, the temperature is measured using a Pt100 platinum resistance temperature sensor. The refrigerant is heated to a predetermined temperature and quality before it enters the test section. In the condenser, the refrigerant flowing from the test section is completely condensed and subcooled. Between the booster pump and the preheating section, there is the refrigerant flowmeter. Pt100 platinum resistance sensors are used to measure the refrigerant temperature at the inlet of the preheating and testing sections, and a pressure gauge measures the absolute pressure. Additionally, a differential pressure gauge is used to measure the total differential pressure. In order to record and store all measured data, a 20-channel data acquisition system is used. Additional details of the experimental setup and procedure are found in (Sun et al. 2010).

Condensation tests were performed at 45 °C (saturation temperature); for mass flux values in the range of 50 to 400 kg/(m^2·s); with an inlet vapor quality of 0.8 and outlet vapor quality of 0.2. Each test point is repeated three times; the deviation between the test data for the three repeated tests is less than 5 %. Moffat (1988) describes how to calculate the uncertainty (%) of directly measured and indirectly obtained parameters; Table 2 summarizes the maximum relative errors of the measurements and calculated parameters. The maximum relative error of the HTC is calculated to be ± 11.32 %.

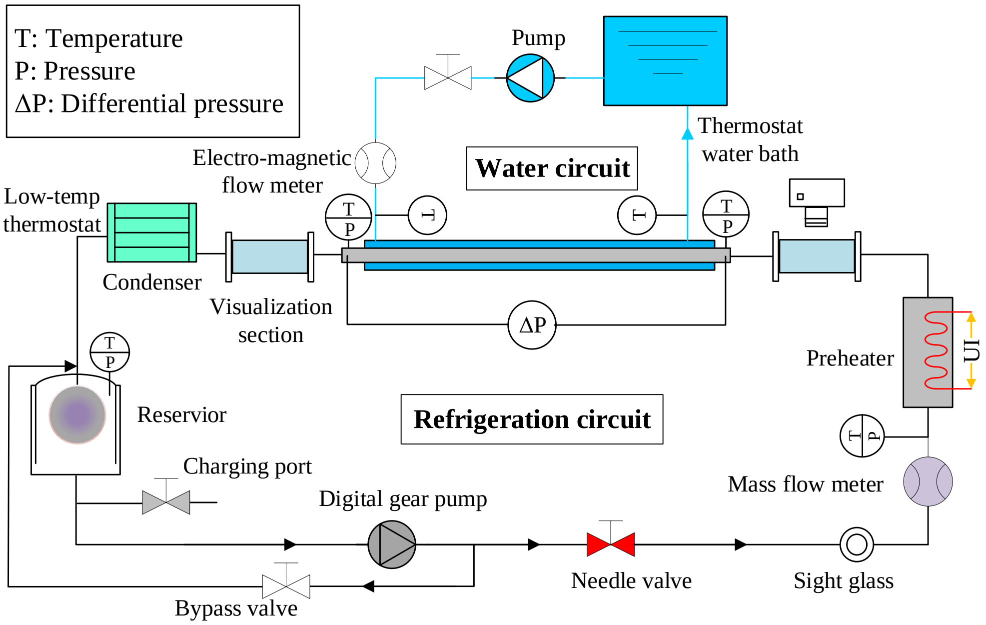

Figure 1: Schematic diagram of the experimental setup

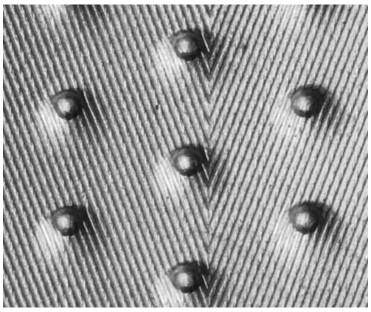

(**a**) EHT-HB/D

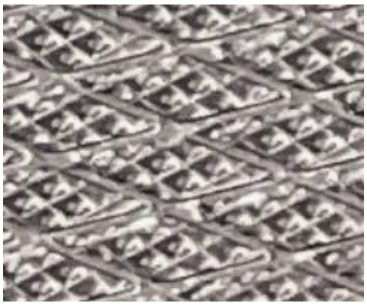

(**b**) 5EHT

Figure 2: Images of the surfaces of the evaluated heat transfer tubes: (a) EHT-HB/D (b) 5EHT

Table 1: Accuracy of the primary and calculated parameters

Primary Parameters	Accuracy
Diameter	± 0.05 mm
Electricity	± 0.1 A
Voltage	± 0.1 V
Length	± 0.5 mm
Temperature	± 0.1 K
Range of Pressure: 0–5,000 kPa	± 0.075 % of full scale
Range Pressure Drop: 0–50 kPa	± 0.075 % of full scale
Range of the Water Flow rate: 0–1,000 kg/h	± 0.2 % of reading
Range of the Refrigerant Flow rate: 0–130 kg/h	± 0.2 % of reading

Calculated parameters	Accuracy
Mass flux, G_{ref}, kg/(m^2·s)	± 1.18 %
Heat flux, kW/m^2	± 2.65 %
Vapor quality, x	± 4.13 %
Evaporation heat transfer coefficient, h (W/m^2·K)	± 10.55 %

3. Results

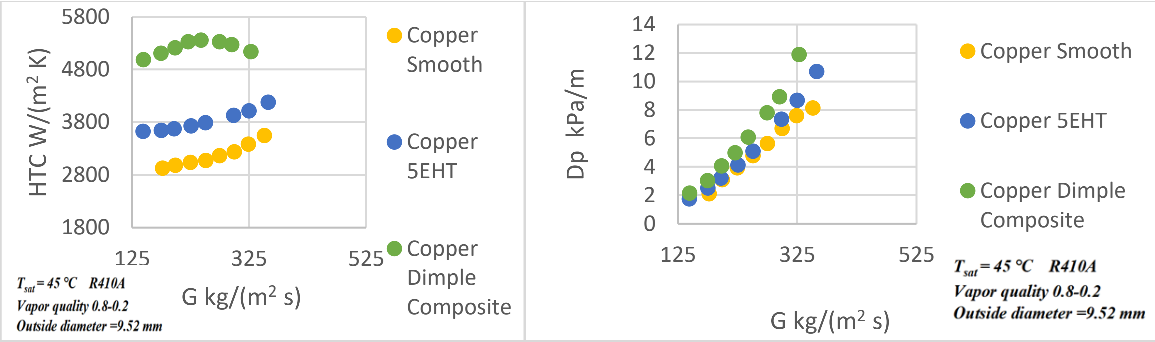

(a) *(b)*

Figure 3: Comparison of tubeside (a) heat transfer coefficient and (b) pressure drop (as a function of mass flow rate) for smooth (ST) and enhanced (5EHT and HX/D) tubes

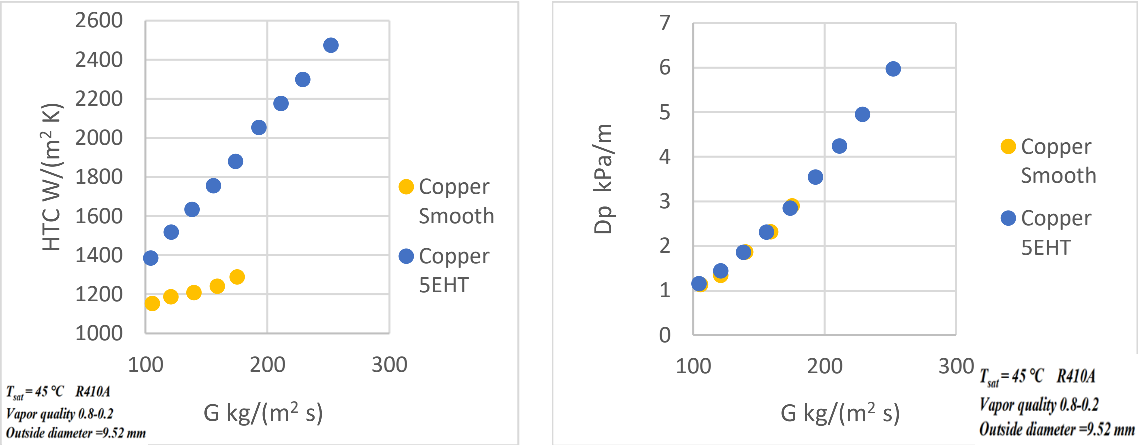

(a) (b)

Figure 4: Comparison of (a) heat transfer coefficient and (b) pressure drop (as a function of mass flow rate) on the outside of smooth (ST) and enhanced (1EHT and HX) tubes

Figure 3 compares the tubeside heat transfer coefficient and pressure drop as a function of mass flow rate for different tubes. Differences in performance between enhancement types is seen; this is a function of differences in the area enhancement ratio between the EHT-HX/D (dimple composite) and 5EHT tubes; additionally, there are differences in the enhancement characters used. The former has higher (area) ratio than the latte. Therefore temperature difference and fin efficiency has a greater effect on performance.

For smooth tubes, with an increase of mass flow rate, the heat transfer coefficient continues to rise; and in the middle region, the increase is relatively slow. However, for the enhanced tube, the heat transfer coefficient initially decreases and then increases; they reach their minimum values near 100 kg/ ($m^2 \times s$). This phenomenon is related to flow pattern, shear force, surface tension, etc., and requires further research.

Figure 4 compares the outside heat transfer coefficient and pressure drop as a function of mass flow rate for different tubes. For both of the tubes evaluated, the heat transfer coefficient increases with an increase of mass flow rate. The Heat Transfer Coefficient (HTC) rate of increase for the 5EHT tube is faster than the HTC increase found for the smooth tube. Differences in performance are a function of differences in the area enhancement ratio and surface structure found in the enhanced tube. The enhanced tube has a higher (area) ratio than the smooth tube. Therefore, temperature difference and fin efficiency have an effect on performance. There is little difference found in pressure drop between tubes.

In order to further compare the performance of enhanced tubes, a heat transfer enhancement factor (EF) is presented in Eq(1). It is defined as the ratio of the HTC of an enhanced tube (h_e) to the HTC for a smooth tube (h_s) under the same working conditions:

$$EF = h_e/h_s \tag{1}$$

where h_e is the heat transfer coefficient of an enhanced tube and h_s is the heat transfer coefficient of a smooth tube.
Figure 5a compares the heat transfer enhancement factor (EF) for tubeside condensation of the enhanced tubes that were evaluated in this study. The heat transfer enhanced factor of the EHT-HB/D tube (1.52-1.76) is the highest, followed by the 5EHT (1.18-1.24) and smooth tubes. Both are greater than 1 indicating increased performance.
An additional dimensionless parameter that combines heat transfer performance and pressure drop can also be used to evaluate the thermal performance of a tube; performance factor (PF) is the enhanced heat transfer ratio (between enhanced and smooth tubes) divided by the pressure drop ratio. Eq(2) is used to calculate PF:

$$PF = (h_e/h_s) \times (p_s/p_e) \tag{2}$$

where p_e is the frictional pressure drop of the enhanced tubes and p_s is the frictional pressure drop of the smooth tubes under the same working conditions.
Figure 5b presents the tube side performance factor of the evaluated enhanced tubes. The performance factor of the EHT-HB/D (.98 – 1.38) and 5EHT tubes (.9 - 1.19) is greater than 1 (except at the highest flowrates). This indicates that the surface structure can ensure high heat transfer performance and low frictional pressure drop.
Figure 6a compares the heat transfer enhancement factor (EF) for condensation on the outside of the tubes that were evaluated in this study. The EF of the 5EHT tube (1.20 – 1.46) is greater than 1, indicating increased performance. Figure 6b presents the performance factor for condensation on the outside of the 5EHT-enhanced tube. The performance factor of the 5EHT tube (1.17 – 1.46) is greater than 1, indicating that the 5EHT surface structure can ensure high heat transfer performance and low frictional pressure drop. It should be noted that all enhanced tubes do not produce results greater than 1. Sometimes, the pressure drop penalty is larger than the enhanced heat transfer that the surface provides. Therefore, PF is a good indicator of the true performance of a tube.

4. Conclusions

Condensation heat transfer process (tubeside and outside surface) of R410a in smooth, herringbone microgrooves with dimple (HB/D), and three-dimensional 5EHT enhanced tubes were studied experimentally. Results include changes in the condensation heat transfer coefficient and pressure drop as a function of mass flux; these results are new and fills the data gap that exists for these types of tubes. The following conclusions can be made from the results obtained:
(1) Tubeside heat transfer enhancement factor (EF) of EHT-HB/D tube is the highest (max 1.76); its performance is closely related to increasing fluid disturbance and improving drainage. Performance factor (PF) of the EHT-HB/D tube (max 1.38) is the highest for most of the flowrates. All this indicating excellent thermal performance.
(2) Best overall condensation heat transfer-resistance characteristics (and highest PF) are shown in the EHT-HB/D tube; it has low friction pressure drop and high heat transfer performance.

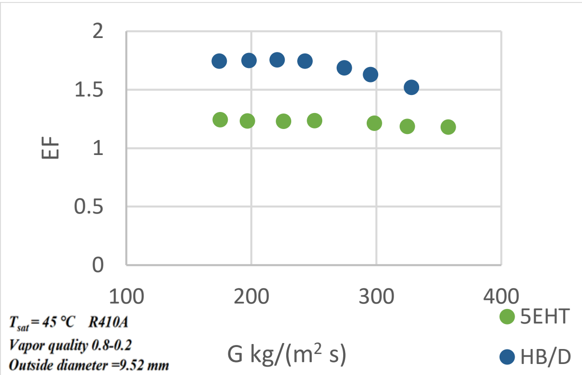

(a) Comparison of the enhancement factors

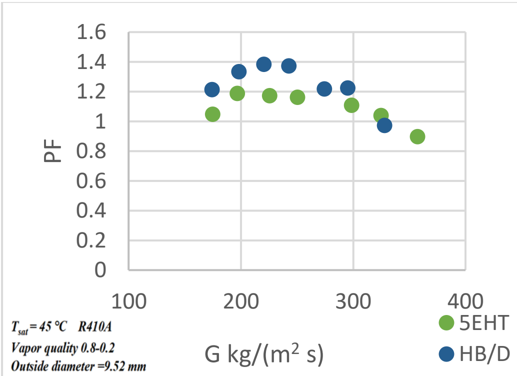

(b) Comparison of performance factors

Figure 5: Comparison of the tube performance for tubeside condensation for the evaluated enhanced tubes

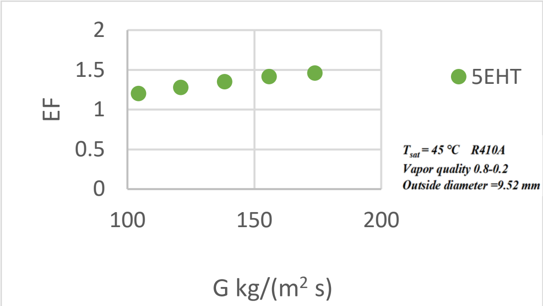

(a) Enhancement factors

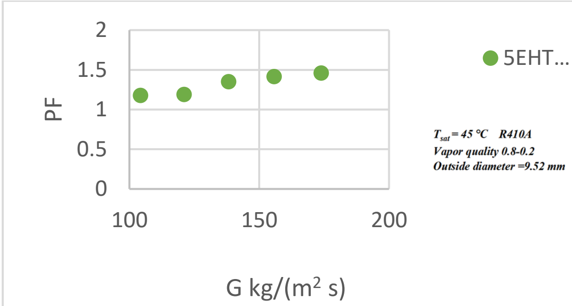

(b) Performance factors

Figure 6: Tube performance for condensation on the outside of the 5EHT enhanced tube

References

Diani A, Campanale M, Rossetto L., 2018, Experimental study on heat transfer condensation of R1234ze(E) and R134a inside a 4.0mm OD horizontal microfin tube. International Journal of Heat and Mass Transfer, 126, 1316-1325.

Gu Y.H., Liao Q., Cheng M., Ding Y., Zhu X., 2020, Condensation heat transfer characteristics of moist air outside a three dimensional finned tube. International Journal of Heat and Mass Transfer, 158, 119983.

Kukulka D.J., Smith R., Li W., 2014, Condensation and Evaporation Characteristics of Vipertex 1EHT Enhanced Heat Transfer Tubes. Chemical Engineering Transactions, 39, 727-732.

Kukulka D.J., Smith R., Li W., 2019, Experimental Comparison of the Evaporation and Condensation Heat Transfer Coefficients on the Outside of Enhanced Surface Tubes with Different Outer Diameters. Chemical Engineering Transactions, 76, 31-36.

Kukulka D.J., Smith R., Li W., 2022, Heat Transfer Performance of Microfin Tubes and Three-Dimensional Heat Transfer Tubes. Chemical Engineering Transactions, 94, 265-270.

Kukulka D.J., Smith R., 2013, Thermal-hydraulic performance of Vipertex 1EHT enhanced heat transfer tubes. Applied Thermal Engineering, 61(1), 60-66.

Laohalertdecha S., Wongwises S., 2011, Condensation heat transfer and flow characteristics of R-134a flowing through corrugated tubes. International Journal of Heat and Mass Transfer, 54(11-12), 2673-2682.

Li G., Huang L., Tao L., 2017, Experimental investigation of refrigerant condensation heat transfer characteristics in the horizontal microfin tubes. Applied Thermal Engineering, 123, 1484–1493.

Li W., Tang W., Gu Z., Guo Y., Ma X., Minkowycz W., He Y., Kukulka D.J., 2020, Analysis of condensation and evaporation heat transfer inside 3-D enhanced tubes. Numerical Heat Transfer Applications, Part A: Applications, 78, 525-540.

Moffat R.J., 1988, Describing the uncertainties in experimental results. Experimental Thermal and Fluid Science, 1(1), 3-17.

Sun Z.C., Li W., Ma X., Ma L., Yan H., 2019, Two-phase heat transfer in horizontal dimpled/protruded surface tubes with petal-shaped background patterns. International Journal of Heat and Mass Transfer, 140, 837-851.

Tang W., Sun Z.C., Li W., 2020, Visualization of flow patterns during condensation in dimpled surface tubes of different materials. International Journal of Heat and Mass Transfer, 161, 120251.

Webb R.L., Kim N.H., 2005, Principles of enhanced heat transfer, 2nd Ed., CRC Press, Boca Raton, FL, United States, 320-400.

Zhao C., Ji W., Jin P., Zhong Y., Tao W., 2017, The influence of surface structure and thermal conductivity of the tube on the condensation heat transfer of R134a and R404A over single horizontal enhanced tubes. Applied Thermal Engineering, 125, 1114–1122.

Zhang J., Zhou N., Li W., Luo Y., Li S., 2018, An experimental study of R410A condensation heat transfer and pressure drops characteristics in microfin and smooth tubes with 5 mm OD. International Journal of Heat & Mass Transfer, 125, 1284–1295.